Our observations suggest that ice shelves close to the climatic limit for existence may disintegrate rapidly. During the next years, increased attention should be paid to the section of the LIS south of Seal Nunataks, which may be subject to major changes if the warming continues. In November 1994, we observed a transverse rift ~50 km in length in section 1, ~30 km inland from the ice front.

REFERENCES AND NOTES

1. C. Swithinbank, *U.S. Geol. Surv. Prof. Pap. 1386-B* (1988).
2. S. S. Jacobs, H. H. Helmer, C. S. M. Doake, A. Jenkins, R. M. Frolich, *J. Glaciol.* **38**, 375 (1992).
3. A. Jenkins and C. S. M. Doake, *J. Geophys. Res.* **96**, 791 (1991).
4. J. H. Mercer, *Nature* **271**, 321 (1978).
5. C. S. M. Doake and D. G. Vaughan, *ibid.* **350**, 328 (1991).
6. P. Skvarca, *Ann. Glaciol.* **20**, 6 (1994).
7. C. S. M. Doake, *ibid.* **3**, 77 (1982).
8. P. Skvarca, *ibid.* **17**, 317 (1993).
9. The ERS-1 SAR images were acquired at the German receiving station near the Chilean Antarctic Base O'Higgins, operating on a campaign basis. The northern LIS was imaged by ERS-1 SAR in July 1992, between December 1992 and February 1993, in August 1993, and between mid-January and mid-February 1995. For comparison with conditions previous to the accelerated retreat, we analyzed Landsat Multispectral Scanner (MSS) images from 1 March 1986.
10. We obtained the ERS-1 SAR data in Universal Transverse Mercator projection based on the WGS-84 ellipsoid with nominal spatial resolution of 25 m by 25 m and location accuracy of better than 100 m in areas of low relief. We used geodetic field data to control and improve the absolute location accuracy. Geometric accuracy was high only close to sea level, because terrain-induced distortions resulting from radar imaging geometry could not be corrected because of a lack of high-resolution elevation data.
11. Data on ice motion, surface mass balance, and ice thickness were obtained for sections 1, 2, and 3 during field observations beginning in the early 1980s. Mean annual velocities from 1984 to 1994 in the center of the profiles (Fig. 2) were 385 m/year in section 1 and 248 m/year in section 3. Ice thicknesses at the same points were 250 m (section 1) and 220 m (section 3).
12. D. A. Peel, in *The Contribution of the Antarctic Peninsula to Sea Level Rise*, E. M. Morris, Ed. (British Antarctic Survey, Cambridge, 1992), pp. 11–15.
13. W. M. Sackinger, M. O. Jeffries, H. Tippens, F. Li, M. Lu, *Ann. Glaciol.* **12**, 152 (1989).
14. N. Contreras, unpublished data.
15. The value of 320 km^2 was derived from an image of the Advanced Very High Resolution Radiometer (AVHRR) of the NOAA satellite with 1-km spatial resolution, acquired on 22 March 1995. An ERS-1 image from 11 February 1995, covering the area around Seal Nunataks, shows the southern ice boundary close to the position of 22 March.
16. Because of a lack of images, the exact date of the final opening of Prince Gustav Channel is not known.
17. T. Hughes, *J. Glaciol.* **29**, 98 (1983).
18. Surface mass balance was determined from measurements at stakes and snow pits. The specific mass balance is the change of mass per unit area within a given time period (the algebraic sum of accumulation and ablation). Mass balance for an entire glacier or ice shelf represents the overall change in mass.
19. The specific mass balance averaged over sites 15, 25, and 35 km south of Seal Nunataks revealed the following temporal changes: 1980 to 1988, 220 mm/year; 1988 to 1991, 130 mm/year; and 1991 to 1994, −70 mm/year.
20. J. C. King, *Int. J. Climatol.* **14**, 357 (1994).
21. J. A. J. Hofmann, in *Actas, Primera Conferencia Latinoamericana sobre Geofísica, Geodesia e Investigación Espacial Antárticas,* Buenos Aires, 30 July to 3 August 1990, p. 160 (1991).
22. P. Skvarca, H. Rott, T. Nagler, *Ann. Glaciol.* **21**, 291 (1995).
23. The following conditions for stability [J. Oerlemans and C. J. van der Veen, *Ice Sheets and Climate* (Reidel, Dordrecht, Netherlands, 1984), pp. 41–64] were no longer valid after the retreat of the LIS along Sobral Peninsula: (i) The gradient thickness H along a flow line in direction x for a stable ice shelf in an embayment with two parallel sides is given by

$$\frac{\partial H}{\partial x} = \frac{\tau_s}{\rho_i g[1 - (\rho_i/\rho_w)]W}$$

where τ_s is the shear stress at the sidewalls, g is the acceleration of gravity, ρ_i and ρ_w are the density of ice and water, respectively, and W is the width of the ice shelf. When the ice front retreated into the bay west of Sobral Peninsula, W became enlarged suddenly, violating the stability criterion. (ii) The shear strain $(\partial u/\partial y + \partial v/\partial x)$ at a stable ice front is zero, where u is the velocity in direction x of the flow line and v is the velocity in direction y. This essentially means that the front is perpendicular to the flow lines. After 1986, the ice front north of Lindenberg Island differed increasingly from this stable geometry.
24. R. A. Bindschadler, M. A. Fahnestock, P. Skvarca, T. A. Scambos, *Ann. Glaciol.* **20**, 319 (1994).
25. A wind velocity of 49 knots results in a surface stress due to wind shear of ~1 N m^{-2}. For an undisturbed ice shelf of the size of the LIS, this force would be ~0.1 to 0.2% of the stress due to shear at the sidewalls. For the breakup of a heavily disturbed ice shelf, even these small forces due to wind may play a role, as may the effects of wind on ocean circulation. An increased probability of calving events during periods of persistent offshore winds and air temperatures above 0°C has been reported for Arctic ice shelves [M. O. Jeffries, *Rev. Geophys.* **30**, 245 (1992)].
26. H. Rott, K. Sturm, H. Miller, *Ann. Glaciol.* **17**, 337 (1993); H. Rott and C. Mätzler, *ibid.* **9**, 195 (1987).

27. The ERS-1 SAR data (from ERS-1 Experiment AO1.A2 and ERS-1/ERS-2 Experiment AO2.A101) were provided by the European Space Agency. The temperature data from Marambio station were provided by Servicio Meteorológico Nacional, Fuerza Aérea Argentina. This work is a contribution to Austrian Science Fund (FWF) Project 10709-GEO, to the National Space Research Program of the Austrian Academy of Sciences, and to the Larsen Ice Shelf Project of Instituto Antártico Argentino, Direcciòn Nacional del Antártico.

5 September 1995; accepted 14 November 1995

DNA: An Extensible Molecule

Philippe Cluzel, Anne Lebrun, Christoph Heller,* Richard Lavery, Jean-Louis Viovy, Didier Chatenay,† François Caron‡

The force-displacement response of a single duplex DNA molecule was measured. The force saturates at a plateau around 70 piconewtons, which ends when the DNA has been stretched about 1.7 times its contour length. This behavior reveals a highly cooperative transition to a state here termed S-DNA. Addition of an intercalator suppresses this transition. Molecular modeling of the process also yields a force plateau and suggests a structure for the extended form. These results may shed light on biological processes involving DNA extension and open the route for mechanical studies on individual molecules in a previously unexplored range.

Many biologically important processes involving DNA are accompanied by deformations of the double helix, and the ability of DNA to stretch "like a spiral spring in tension" (*1*, p. 739) was recognized long ago (*1–3*). The mechanics of DNA has regained interest in recent years as a result of the possibility of working with individual molecules. The extension of a duplex DNA molecule under the action of an external force was measured by Smith *et al.* (*4*) and compared to predictions of the wormlike chain model (*5*). In good agreement with this theory, these researchers observed that a force of 2 to 3 pN is able to stretch the DNA to 90% of its contour length at rest in the B-form, l_0, and that the force then rises sharply when the extension approaches l_0. This experiment was restricted to forces smaller than 20 to 30 pN, whereas it has been suggested that DNA is able to withstand about 500 pN before breaking (*6*). We present here a study of the force-extension response of a single duplex DNA molecule submitted to forces ranging from 10 to 160 pN, using an apparatus (Fig. 1) that improves on that developed by Kishino and Yanagida to study the actin-myosin interaction (*7*).

We repeated our experiment many times using different fibers and stretching velocities (a few seconds was typically required for stretching). Two types of curves were ob-

P. Cluzel, C. Heller, J.-L. Viovy, Institut Curie [URA Centre National de la Recherche Scientifique (CNRS) 448 and 1379], 11–13 Rue Pierre et Marie Curie, Paris 75005, France.
A. Lebrun and R. Lavery, Laboratoire de Biochimie Théorique (URA77 CNRS), Institut de Biologie Physico-Chimique, 13 Rue Pierre et Marie Curie, Paris 75005, France.
D. Chatenay, LUDFC, Institut de Physique, 3 Rue de l'Université, Strasbourg 67084, France.
F. Caron, Ecole Normale Superieure, Laboratoire de Génétique Moléculaire (URA CNRS 1302), 46 Rue d'Ulm, Paris 75230, France.

*Permanent address: Max-Planck-Institut für Molekulare Genetik, Ihnestraße 73, D-14195 Berlin-Dahlem, Germany.
†Present address: Rockefeller University, Box 265, 1230 York Avenue, New York, NY 10021, USA.
‡To whom correspondence should be addressed.

tained. The first was a simple and monotonic profile with one plateau followed by a steep drop in force (Fig. 2A). The other type of curve was complex and irreproducible with several plateaus (Fig. 2B). We performed the experiment with a variable number of DNA molecules grafted on one bead. High grafting densities led to complex, irreproducible curves, whereas the simple profiles were mostly encountered with a low grafting density of about one to two DNA molecules per bead. Such profiles were reproducible typically to within <10 pN and <2 μm between different experiments, irrespective of the pulling velocity, and by repeated stretching during a single experiment. We therefore attribute the simple profile to a single DNA molecule and the complex ones to multiple grafting.

The DNA was able to stretch to at least 1.7 times its B-form contour length l_0 (Fig. 2A). This observation is in agreement with that of Bensimon *et al.* (6), who reported extensions as large as 2.1 (l_0) under the action of a receding meniscus. These results are also in agreement with those of Smith *et al.*, who reported a 1.85 times extension of DNA pulled between two pipettes (8).

Our most important result is the presence of a plateau where the DNA molecule stretches at almost constant force; this finding appears to agree with preliminary results of Smith *et al.* (8) obtained by manipulating DNA with optical tweezers, although more detailed evidence will be needed to confirm this point. Because the plateau begins close to the fully extended length of the B form, we interpret it as a tension-induced structural transition. Qualitatively, this process is a reversible transformation of bases from the B form to a stretched structure (hereafter termed S), which is complete at the end of the plateau.

Further insight into this transition can be gained with the use of a simplified representation of DNA as a chain of elements (nucleotide pairs) with two states: a short one with length l_1 (B-DNA) and a long one with length l_2 (S-DNA), with an energy difference (ΔE) between the states. ω is the nearest neighbor interaction between adjacent B and S elements and determines the energy for inserting an S-form element within a B-form section. A similar two-state model has already been proposed to describe the helix-coil transition of polypeptides and has been solved exactly (9). The force can be represented as follows:

$$f = \Delta E/\Delta l + (kTN/\Delta l)\ln[(\beta + 2y/\Delta l)/(\beta - 2y/\Delta l)] \quad (1)$$

where

$$\beta = \sqrt{1-[1-\exp(+\omega/kT)][1-(2y/\Delta l)^2]} \quad (2)$$

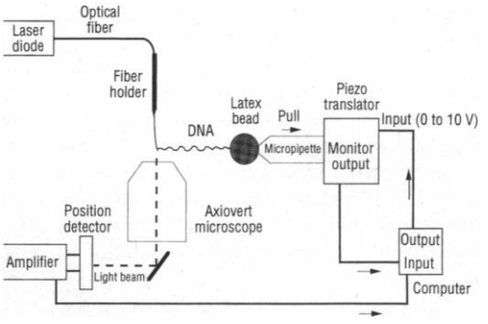

Fig. 1. Experimental apparatus. The force sensor is a monomode optical fiber placed in the experimental cuvette and held vertically with the use of a rigid tube to avoid meniscus effects at the liquid surface. A covering layer of polydimethylsiloxane (molecular weight, 2000) was used to avoid water evaporation. We adjusted the stiffness of the fiber (10^{-2} to 10^{-4} N/m) by choosing its length and its diameter, using controlled chemical degradation of its outer layer. It was calibrated by a measurement of bending during uniform translation in water solution (*17*). The optical fiber was fed by a laser diode (Power Technology, 7 mW), and the motion of its tip, once amplified by a modified inverted microscope (Zeiss Axiovert), was detected by a position-sensitive photo-diode (Silicon Detector). A displacement resolution of about 10 nm was obtained. The DNA molecule is attached specifically at one end to the fiber and at the other to a microbead (*18*). The bead was caught and maintained at the tip of a rigid micropipette by creating a weak drop in pressure. The micropipette was then driven away from the fiber by a computer-controlled piezo-translator stage (PI Instruments), and the fiber deflection was recorded (National Instrument software, Labview). The coupling between the displacement of the pipette and the bending of the fiber was principally due to the linked DNA molecule, although a weak contribution (<20 pN) from hydrodynamic backflow was present for large pipette velocities. When necessary, we subtracted this perturbation by performing a blank experiment with an identical pipette displacement, after deliberately breaking the DNA link.

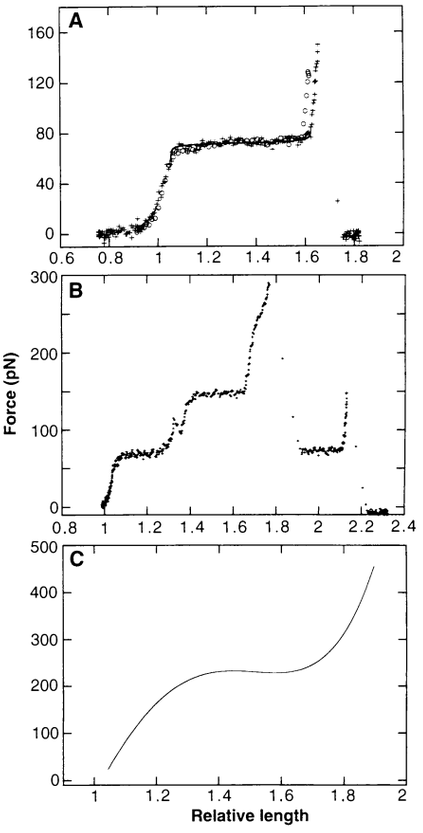

Fig. 2. (**A**) Two examples of force versus extension profiles for EMBL3 λ DNA (*18*) [contour length, 15.1 μm (*16*)] in phosphate-buffered solution (100 mM; 80 mM Na^+ and 0.01% Tween) obtained with different fibers and using pulling velocities of 1 and 10 μm/s (symbols "o" and "+," respectively). For clarity, only a subset of data is plotted. The first 10 μm of the displacement is not represented because it is indistinguishable from background noise (*19*). By repeatedly pulling the pipette to distances up to 20 μm and returning it to its starting position, the same curve could be followed within an experimental error of <2 pN. In contrast, the abrupt drop in force could be observed only once for a given molecule, and subsequent tractions lead only to a very weak displacement of the fiber because of the hydrodynamic backflow of the pipette. The accuracy of the backflow correction in the + curve above was verified by comparison with the o curve obtained by slow pulling and without correction. We associate the irreversible event with the rupture of the DNA-fiber or the DNA-bead links because the force at rupture is smaller than the force required to break duplex DNA (*6*) and is similar to the force recently reported for the rupture of a biotin-avidin association (*20*). The full line shows the best fit obtained with Eq. 1 for $\omega = -16.6 \pm 0.9$ kJ/mol per base pair, $(l_2 - l_1) = 1.96 \pm 0.2$ Å, and $\Delta E = 8.4 \pm 0.5$ kJ/mol per base pair. (**B**) Force versus extension profile obtained when several DNAs were grafted between the bead and the fiber [all other conditions were identical to those in (A)]. The complexity of the curve arises from the fact that the molecules were not grafted at the same position and therefore did not, in general, undergo stretching or rupture for the same bead displacement. In contrast with the simple curves obtained with a single DNA molecule (A), such curves could not be not reproduced when the pipette was pulled repeatedly. (**C**) Force of stretching derived from a polynomial fit to the deformation energy from modeling (see Fig. 4). The extent of the plateau is consistent with the observations in (A). The force at the plateau (240 pN) was obtained by stretching with the total twist per turn held constant. If the twist is allowed to vary, the force drops to 140 pN (note that the biochemical design of the experiment, in principle, allows DNA to rotate freely at one end during stretching, so that complementary experiments with the two ends torsionally blocked will be interesting). Exact agreement with experiment cannot be expected because of the simplified representation of DNA and its environment—notably involving imposed helical symmetry, regular base sequences, and the absence of thermal agitation.

where k is the Boltzmann constant, T is the temperature in kelvin, $y = x/N - (l_1 + l_2)/2$, N is the number of elements (nucleotide pairs), $\Delta l = (l_2 - l_1)$, and x is the extension of the chain (in micrometers). Poor fits are obtained for $\omega \rightarrow 0$. Taking ω equal to -16.6 kJ/mol per base pair, which disfavors isolated S-form or B-form elements and implies a cooperative transition, leads to an excellent fit (*10*) (see full line in Fig. 2A).

If, as suggested above, the plateau is the result of a DNA conformational transition, a drastic change could be expected in the presence of intercalating agents. The transition indeed disappears in the presence of 10 μg/ml of ethidium bromide (Fig. 3). At the present stage, one can note the following: First, the rise of the force with extension is smoother than shown in Fig. 2A, both before or after the plateau. This may be a result of exchange of the intercalator during the stretching process. Second, the force rises at a larger value of the extension than without an intercalator, in agreement with the well-known lengthening and unwinding of DNA induced by intercalating agents and with earlier observations by Smith *et al.* (*4*).

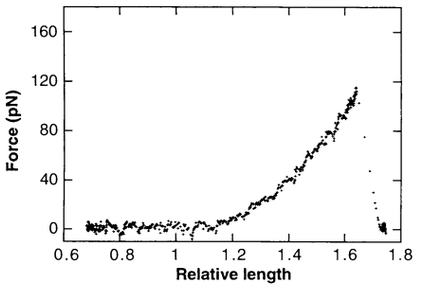

Fig. 3. Force versus extension curve in the presence of 10 μg/ml of ethidium bromide at a pulling rate of 10 μm/s, other conditions being identical to those of Fig. 2A. The relative length is again defined with respect to the B-form contour length (15.1 μm).

Molecular modeling of the DNA stretching process, performed with the program JUMNA (Fig. 4), also leads to a plateau in the force-displacement curve (Fig. 2C). The structure of the S form, modeled by stretching the ends of one strand of the duplex (compatible with our experiment here), suggests that extension involves a reduction in helical diameter and a strong base pair inclination that maintains both base stacking and pairing until a relative length of 2.0. This finding correlates with early spectroscopic studies by Fraser and Fraser on stretched DNA fibers (*11*). The strong base inclination induced by stretching suggests an explanation for the cooperative nature of the transition, because discontinuities in inclination would imply a loss of base stacking or would require DNA kinking.

The 1.6 times extension of DNA at the end of the force plateau is close enough to the extension induced by RecA fixation (*12, 13*) to speculate on the biological importance of an extended form of isolated DNA. The purpose of extending and unwinding DNA, in the case of RecA, is to facilitate the formation of a triplex (*14*), which is a putative intermediate during recombination. A pre-extended DNA form may be an intermediate step in such triplex formation. The role of RecA might thus be to induce such a transition by means of specific interactions between the protein and the extended form.

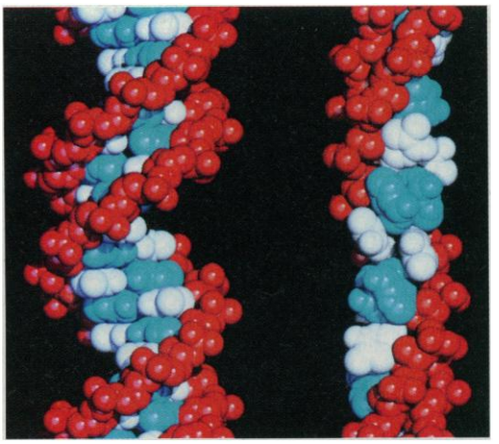

Fig. 4. DNA stretching was modeled with use of the JUMNA molecular mechanics program developed for studying nucleic acid conformations (*21–23*). An all-atom force field is used, and efficient minimization is allowed by a reduced variable representation involving helicoidal and internal variables (bond rotations and valence angles). Solvent and counterion effects are represented by a distance-dependent dielectric function and reduced phosphate charges. An infinite DNA polymer was studied with the use of helical symmetry constraints and a repeat of 10 nucleotide pairs. Stretching involved minimizing the energy per turn of the polymer as a function of the length of one of its strands (imposed with a quadratic distance constraint between C5′ and C3′ atoms separated by 10 nucleotides). Results are presented for an alternating AT sequence. The figure shows space-filling graphics of the relaxed linear DNA (left) and DNA stretched by a factor of 1.7 (right). The elongated DNA is characterized by a strong base pair inclination, a narrow minor groove, and a diameter roughly 30% less than that of B-DNA. The base pairs, which are exposed on the major groove side of the double helix, are still bound by a single hydrogen bond, and strong interstrand stacking between adenines can be seen. This conformational change occurs progressively and cooperatively during stretching. Modeling, however, indicates that the final conformation and the energetics of stretching depend both on base sequence and on which strand termini are tethered during stretching.

REFERENCES AND NOTES

1. M. H. F. Wilkins *et al.*, *Nature* **171**, 738 (1953).
2. M. H. F. Wilkins *et al.*, *ibid.* **167**, 759 (1951).
3. F. H. C. Crick and J. D. Watson, *Proc. R. Soc. London Ser. A* **223**, 80 (1954).
4. S. B. Smith *et al.*, *Science* **258**, 1122 (1992).
5. C. Bustamante *et al.*, *ibid.* **265**, 1599 (1994); A. Vologodskii, *Macromolecules* **27**, 5623 (1994); J. Marko and E. D. Siggia, *ibid.*, **28**, 8759 (1995).
6. D. Bensimon *et al.*, *Phys. Rev. Lett.* **74**, 4754 (1995); A. Bensimon *et al.*, *Science* **265**, 2096 (1994).
7. A. Kishino and T. Yanagida, *Nature* **334**, 74 (1988).
8. S. B. Smith *et al.*, *Biophys. J.* **68**, A250 (1995).
9. T. L. Hill, *J. Chem. Phys.* **30**, 383 (1959); B. Zimm and J. Bragg, *ibid.* **31**, 526 (1959).
10. Because this simple model does not take into account the entropic elasticity, it becomes rapidly inaccurate for extensions outside the plateau region. For a complete description, a theory taking into account the degrees of freedom related to the exchange between states, as well as those related to entropic elasticity (*5*), will be required. Additional elasticity may also arise from distortions of bond angles (*15*) or from a dependence of transition energies on base pair content and sequence.
11. M. J. Fraser and R. D. B. Fraser, *Nature* **167**, 760 (1951).
12. A. Stasiak and E. diCapua, *ibid.* **299**, 185 (1982).
13. M. M. Cox and I. R. Lehman, *Annu. Rev. Biochem.* **56**, 229 (1987).
14. B. J. Rao, M. Dutreix, C. M. Radding, *Proc. Natl. Acad. Sci. U.S.A.* **88**, 2984 (1991).
15. J. L. Viovy, C. Heller, F. Caron, Ph. Cluzel, D. Chatenay, *C. R. Acad. Sci. Paris* **317**, 795 (1994).
16. A.-M. Frischauf, H. Lehrach, A. Poustka, N. Murray, *J. Mol. Biol.* **170**, 827 (1983).
17. R. G. Cox, *J. Fluid Mech.* **44**, 791 (1970).
18. EMBL3 λ DNA (*16*) was labeled at the right end for attachment to a polystyrene microbead (Polyscience; 2.8 μm) covered with antibody to digoxigenin (anti-DIG) by ligation of a modified 12-mer oligonucleotide, complementary to the 5′ protruding right end of λ DNA. The modification consists of labeling the oligonucleotide with terminal transferase in the presence of DIG 2′3′-dideoxyuridine-5′-triphosphate (Boehringer). At the left end, DNA was multilabeled (about 150 ligands) on both strands with biotin by the ligation, by means of an adapter, of a 700–base pair fragment labeled with biotin by the polymerase chain reaction.
19. The exact value of the initial extension, which is related to the position of the bead with respect to the anchoring of DNA on the fiber, is known only to within 3 μm; therefore, internal reference with a 1-μm accuracy was obtained by fitting the steep rise of the entropic force at the vicinity of the full contour length extension (*4, 5*). This fit yields a persistence length smaller than that obtained by others (*5*) by a factor of 3 to 4. This decrease is qualitatively consistent with our use of a higher salt concentration, but a quantitative study of salt effects would require a higher accuracy in the low-force domain and is beyond the scope of our work here.
20. E.-L. Florin, V. T. Moy, E. Gaub, *Science* **264**, 415 (1994).
21. R. Lavery, in *Structure and Expression*, vol. 3 of *DNA Bending and Curvature*, W. K. Olson, R. H. Sarma, M. H. Sarma, M. Sundaralingam, Eds. (Adenine Press, New York, 1988), pp. 191–211.
22. R. Lavery, K. Zakrzewska, H. Sklenar, *Comput. Phys. Commun.* **91**, 135 (1995).
23. R. Lavery, *Adv. Comput. Biol.* **1**, 69 (1994).

24. The authors acknowledge support from the Chemistry Department of the CNRS, the Ultimatech program, the DRET/Ministère des Armées, the European Economic Community Biomed Program, and the French Supercomputing Centre IDRIS. We thank J. Malthête and J. Davidovits for helpful discussions concerning the chemistry of these experiments, A. Laigle for helpful preparatory experiments, and F. Breton for technical assistance.

15 September 1995; accepted 15 November 1995